Heat induced evaporative antisolvent nanoprecipitation (HIEAN) of itraconazole

Mugheirbi Naila Abdulhamid, Paluch Krzysztof Jan, Tajber Lidia*

School of Pharmacy and Pharmaceutical Sciences, Trinity College Dublin, Dublin 2, Ireland.

*To whom correspondence should be addressed: lidia.tajber@tcd.ie, Phone: 00353 1 896 2787

Fax: 00353 1 896 2810

KEYWORDS: Itraconazole, poly(ethylene glycol), methoxylated poly(ethylene glycol), antisolvent evaporative nanoprecipitation, nanoparticles, amorphous.

Abstract

Itraconazole (ITR) is an antifungal drug with a limited bioavailability due to its poor aqueous solubility. In this study, ITR was used to investigate the impact of nanonisation and solid state change on drug's apparent solubility and dissolution. A bottom up approach to the production of amorphous ITR nanoparticles (NPs), composed of 100% drug, with a particle diameter below 250 nm, using heat induced evaporative antisolvent nanoprecipitation (HIEAN) from acetone was developed. The NPs demonstrated improved solubility and dissolution in simulated gastro-intestinal conditions when compared to amorphous ITR microparticles. NPs produced with polyethylene glycol (PEG) or its methoxylated derivative (MPEG) as a stabiliser enabled the production of smaller NPs with narrower particle size distribution and enhanced apparent solubility. MPEG stabilised NPs gave the greatest ITR supersaturation levels (up to 11.6 ± 0.5 µg/ml) in simulated gastric fluids. The stabilising polymer was in an amorphous state. Dynamic vapour sorption data indicated no solid state changes in NP samples with water vapour at 25 °C, while crystallisation was apparent at 50 °C. HIEAN proved to be an efficient method of production of amorphous ITR NPs, with or without addition of a polymeric stabiliser, with enhanced pharmaceutical properties.

1. Introduction

The increasing frequency of drug candidates with complex molecular structure and limited aqueous solubility is a major challenge to the pharmaceutical industry. The poor solubility of these drugs in the gastro-intestinal fluid is a substantial hurdle to their oral administration. Many therapeutically active compounds exhibiting dissolution rate-limited bioavailability fail commercialisation, which endeavours scientists to establish a number of strategies to improve the solubility and subsequent bioavailability of such drugs (Dressman et al. 2000, Gardner et al. 2004). Production of nanoparticles (NPs) is one of the commonly investigated approaches to improve the performance of drugs that possess high permeability but poor solubility (BSC class II drugs) and are likely to have dissolution-limited absorption rates. The breakdown of bulk material into particles in the nanometre range leads to a significant increase in the surface area and thus an improvement in dissolution rates (Liversidge et al. 1992).

Itraconazole (ITR) is a BCS class II drug with aqueous solubility of less than 1 μg/ml (Matteucci et al. 2009), which has been extensively used as a model drug to study the potential advantages of nanonisation. It is an azole antifungal agent, which is effective against a variety of fungal species such as *Aspergillus*, *Cryptococcus*, *candida*, *Blastomyces*, and *Histoplasma capsulatum var. capsulatum* (Odds et al. 2000, Saag and Dismukes 1988). However, the use of ITR is limited owing to its poor bioavailability and variable absorption (Kapsi and Ayres 2001) where the oral solid dosage form available on the market (Sporanox®) has an absolute bioavailability of 30% (Barrett et al. 2008).

A wide variety of techniques have been used to form ITR NPs. The top down approach is the most commonly used since it is a scalable approach that avoids the use of organic solvents (Liu et al. 2011) which includes wet milling (Lee et al. 2010) and high pressure homogenization (Chen et al. 2008, Owen et al. 2009). The majority of the commercially available NP-based formulations such as Rapamune®, Emend®, TriCor®, Megace®, and Triglide® are produced using these techniques (van Eerdenbrugh et al. 2008). However, they are time and energy consuming methods (Shah 2006, Wiedmann et al. 1997, Yang et al. 2010, Tam et al. 2010). Moreover, the produced NPs are susceptible to contamination from milling media or the homogenization chamber (Chow et al. 2007).

On the other hand, the bottom up approach is simple with relatively low cost and achieved mainly through antisolvent precipitation and solvent evaporation (Badawi et al. 2011, Weers et al. 2007). However, the application of bottom up techniques to industry is relatively challenging owing to the possible presence of organic solvent residues in the final product (Keck and Müller 2006, Chen et al. 2006). Different solvent-antisolvent systems and stabilisers have been investigated for the production of ITR nanocrystals and amorphous NPs via antisolvent precipitation (Dalvi and Dave 2010, Matteucci et al. 2006, Kumar et al. 2009, Beck et al. 2010). Although nanocrystals exhibited an improved solubility and dissolution profile compared to the marketed product (Badawi et al. 2011), amorphous NPs are expected to have superior bioavailability due to the absence of a long-range order and periodicity in their structure (Shah et al. 2006). The formation of NPs involves several steps including supersaturation, nucleation and growth of the formed nuclei for nanocrystals, while supersaturation and precipitation is seen for amorphous NPs. Uncontrolled particle growth may result in the aggregation of NPs.

The size, solid state and purity of the produced particles mainly depend on the rate and degree of the generated supersaturation (Mullin and Nývlt 1971, Jones and Mullin 1974). A quasi-emulsion solvent diffusion method was used by Re and Biscans (1998) to prepare ketoprofen microspheres using acetone as a solvent. Chen et al. (2002) introduced the use of antisolvent phase at high temperature (75 °C) to evaporate the solvent phase during antisolvent precipitation of NPs and this method resulted in the production of 253 nm cyclosporine NPs. The same method was utilised to produce ITR microparticles with rapid dissolution properties (Chen et al. 2004). To the best of our knowledge, no reports of ITZ NPs produced via this method are available in the literature. Bosselmann et al. (2012) demonstrated the production of partially amorphous ITR NPs using advanced evaporative precipitation in hot aqueous solution. The method employed in that study involved several steps and required pre-emulsification of dichloromethane solution of ITR with lecithin in aqueous solution of PVP and sodium deoxycholate.

In this work, we report on the use of a simple heat induced evaporative antisolvent nanoprecipitation (HIEAN) for the preparation of amorphous ITR NPs with and without a polymeric stabiliser. The effect of inclusion of poly(ethylene glycol) (PEG 2000) and its metoxylated derivative (MPEG) as stabilisers in the antisolvent phase was also investigated. The solid-state nature of the produced NPs was determined using thermal analysis and powder X-ray diffraction. The effect of combining size reduction with the conversion into amorphous state on the solubility and dissolution profile of ITR in biorelevant media was examined. Finally, the properties of NPs and the effect of incorporation of PEG and MPEG as stabilisers were assessed using dynamic vapour sorption analysis.

2. Materials and methods

2.1. Materials

Itraconazole (ITR) was a gift from Welding GmbH (Hamburg, Germany). Poly(ethylene glycol) (PEG) and poly(ethylene glycol) methyl ether (MPEG) with average molecular weights of 2,000 were purchased from Aldrich Chemical Co. Ltd. (Dorset, UK). Acetone Chromasolv® HPLC grade was obtained from Sigma-Aldrich (Dorset, UK). Acetonitrile HPLC grade was purchased from Fisher Scientific (Loughborough, UK). Simulated Intestinal Fluid (SIF) powder was acquired from Biorelevant.com Ltd (Croydon, Surrey, UK). Ethanol (≥99.8%) employed in DVS experiments was purchased from Sigma-Aldrich Ltd. (Arklow, Ireland). All other chemicals and solvents were of analytical grade.

2.2. Heat induced evaporative antisolvent nanoprecipitation (HIEAN) of ITR

The antisolvent phase was either pure deionised water or 0.64 mg/ml PEG (2,000) or 1 mg/ml MPEG (2,000) solution in deionised water and maintained at 80 °C. The solvent solution was prepared by dissolving 6.4 mg/ml of ITR in acetone and this solution was maintained at 50 °C. An aliquot of the solvent phase was rapidly injected into the antisolvent phase, that was continuously stirred at 13,000 rpm, using a 0.5 * 16 mm Sterican® needle using conditions (antisolvent phase and composition as well as solvent/antisolvent ratios) presented in Tables 1 and 2. Once the whole volume of the ITR solution was injected, the mixture was immediately transferred to a jacketed cylinder and allowed to cool to 25 °C.

2.3. Spray drying of amorphous microparticles of ITR

Amorphous microparticles (MPs) of ITR were prepared via spray drying using a laboratory scale Buchi B-290 mini Spray Dryer (Buchi LaboratoriumsTechnik AG, Flawil, Switzerland) operating in the open cycle mode configuration using nitrogen as a drying gas. 4% w/v ITR solution in dichloromethane was spray dried using the following parameters: inlet temperature of 40 °C, outlet temperature of 34 °C, atomising gas flow of 40 mm (rotameter setting) corresponding to 473 normL/h, aspirator rate of 100% and a feed flow rate of 25% (10 ml/min).

2.4. Determination of solubility of crystalline ITR

Solubility of the crystalline ITR in acetone at different temperatures (0, 5, 10, 20, 30, 40, and 50 °C) was determined as follows. At each temperature, 100 mg of ITR was added to 10 ml acetone kept in a closed vial and left to equilibrate overnight with a continuous stirring at 1,000 rpm. Each sample was then filtered through a 0.45 µm syringe filter (VWR, Ireland) and the filtrate diluted 200 times using the mobile phase (40% phosphate buffer and 60% acetonitrile v/v, as described in Section 2.5). Solubility of crystalline ITR in water and antisolvent solutions of different stabilisers (PEG 2,000 and MPEG 2,000) at 80 °C and 25 °C was also measured by equilibrating the drug in the antisolvent solution for 2 hours followed by filtration using a 0.45 µm syringe filter (VWR, Ireland). For each sample, 1 ml of the filtrate was then evaporated in a microtube (VWR, Ireland), the residue was dissolved in 300 µl of the mobile phase and then analysed using HPLC (Section 2.5).

Solubility of crystalline ITR in the fasted state simulated gastric fluid (FaSSGF, pH=1.6) and fed state simulated intestinal fluid (FaSSIF, pH=6.5) was assessed by placing 10 mg of the drug in 10 ml of the simulated fluid (prepared according to manufacturer's instructions) at 37 °C and in

each case the mixture was continuously stirred at 1,000 rpm. 2 ml aliquots were withdrawn from each vial after 12 and 24 hr and filtered through a 0.45 µm syringe filter. 0.6 ml of the filtrate was then diluted with 0.4 ml of the mobile phase and analysed using HPLC (Section 2.5).

2.5. High performance liquid chromatography (HPLC)

The concentrations of ITR were measured using a Waters Symmetry® C_{18} 5 µm (4.6*150 mm) column attached to a Waters HPLC system equipped with a Waters 1525 Binary HPLC pump, Waters 717 plus autosampler and operating with a Waters 2487 dual λ absorbance detector (λ=260 nm). For the solubility studies of ITR in acetone, a 50 µl injection volume was used with a flow rate of 2 ml/min for 7 min. For the solubility studies of ITR in the antisolvent phase a 100 µl injection volume was used due to the low solubility of ITR in aqueous solutions. For the dissolution studies, 50 µl injection volumes were used with a flow rate of 1 ml/min for 14 min to prevent ITR peak from overlapping with peaks of the excipients present in the dissolution media. HPLC was also used to detect the quantity of ITR in the PEG and MPEG stabilised NPs and in those experiments a 20 µl injection volume was used.

2.6. Separation, freeze drying and washing of ITR NPs

The formed NP dispersions, as indicated later and except for the directly freeze dried sample (ITRf), were centrifuged at 12,000 rpm at 4 °C for 30 min using an Eppendorf 5810R centrifuge (Hamburg, Germany) (Badawi et al. 2011). The supernatant was removed and NPs in the pellet were frozen in liquid nitrogen and freeze dried at 35 mTorr vacuum pressure and -75 °C for 24 hr using a VirTis Bench Top 6K freeze dryer model EL (SP Scientific, USA). The effect of washing on the NP morphology was studied by washing the residue left after centrifugation with 5 ml

deionised water. The suspension was then recentrifuged and freeze dried using the same conditions as mentioned above. Another sample was prepared and freeze dried without centrifugation to assess the necessity of this step.

2.7. Characterisation of ITR particles

2.7.1. Particle size and morphology

The mean particle size and the polydispersity indices (PDI) of NPs were measured using Zetasizer Nano series (Malvern Instruments, UK). The samples were diluted 1:1 with the antisolvent solution and placed in a ZEN0112 low volume disposable sizing cuvettes. All measurements were carried out at 25 °C with an equilibration time of 2 min. The analysis was performed in triplicate for each sample and the average was recorded along with the PDI values.

A Zeiss Supra variable Pressure Field Emission Scanning Electron Microscope (Germany) equipped with a secondary electron detector and accelerating voltage of 5 kV was used for the morphological examination of ITR particles. Aliquot samples of the nanosuspensions were placed directly on aluminium stubs and dried using nitrogen purge. For the freeze and spray dried samples, powders were placed on carbon tabs fitted on aluminium stubs. The solid samples were sputter coated with gold/palladium under vacuum before analysis.

In an attempt to examine the surface texture of NPs in their native state before coating, helium ion microscopy (HeIM) was used where liquid samples were drop casted onto aluminium stubs, dried using nitrogen purge and examined using a Zeiss Orion plus (Peabody, MA, USA). All

images were acquired using 10 µm aperture and 30 kV accelerating voltage. Beam currents were 0.5 to 0.9 pA. No coating and no charge compensation techniques were used.

2.7.2. Differential scanning calorimetry (DSC)

Accurately weighed samples (7-9 mg) were placed in pin-holed aluminium pans. The DSC measurements were performed using a Mettler Toledo DSC 821e (Greifensee, Switzerland), under nitrogen purge. A temperature range of 25-200 °C was applied with a heating rate of 10 °C/min (Liu et al. 2011). For the spray dried material a 5 °C/min heating rate was also used. The DSC system was controlled by Mettler Toledo STAR^e software (version 6.10). The starting ITR material, the stabilisers and physical mixtures were tested as reference samples. Integration under the crystallisation peak shoulder at around 120 °C (Δh_{cryst}) and the melting endotherm at around 168 °C (Δh_{melt}) were utilised to estimate the percent crystallinity in the produced NPs using the following formula (Eqn. 1, Hancock and Parks 2000):

$$\%\ crystallinity\ = \frac{\Delta h_{melt} - \Delta h_{cryst}}{\Delta h_{meltITR}} \qquad \text{Eqn.1}$$

where $\Delta h_{meltITR}$ is the heat of melting for pure crystalline ITR.

2.7.3. Dynamic vapour sorption

Spray dried ITR and ITR NPs were analysed with a Dynamic Vapour Sorption (DVS) Advantage-1 automated gravimetric vapour sorption analyser (Surface Measurement Systems Ltd., London, UK). The temperature was maintained constant at 25.0 ± 0.1 °C (ethanol or water vapour) or 50.0 ± 0.1 °C (water vapour). The analysis was performed in triplicate for each sample. In all

measurements, around 10 mg of the powder was loaded into a sample net basket and placed in the system. All samples were equilibrated at 0% of RH until constant mass (dm/dt ≤ 0.002 mg/min for at least 10 min). The reference mass was recorded as a mass equilibrated at 0% RH. Samples were then subjected to either ethanol or water vapour sorption/desorption analysis in a range from 0% to 90% of relative pressure (P/P_0) in 10% P/P_0 steps.

Samples recovered following the sorption-desorption cycle were analysed using PXRD and DSC to examine their solid-state properties and to detect the possible crystallisation of drug and/or polymer.

2.7.4. Quantification of ITR in NPs (drug loading)

HPLC (as described in Section 2.5) was used to quantify the amount of ITR in NPs. In these experiments, 1 mg of the produced NPs was dissolved in 10 ml of the phosphate buffer/acetonitrile mobile phase and analysed using HPLC. The stabiliser-free NPs were assumed to have 100% ITR since no stabilisers were used in the preparation of these NPs.

2.7.5. Powder X-ray diffraction (PXRD)

PXRD measurements were performed using a Rigaku Miniflex II, desktop X-ray diffractometer (Japan) equipped with a Cu Kα radiation X-ray source. The samples were mounted on a low-background silicon sample holder and scanned over a 2θ range of 5-40° (Paluch et al. 2010).

2.8. Determination of solubility of ITR nano- and micro-particles

ITR displays pH dependent solubility and dissolution with a very low solubility at high pH (Miller et al. 2012), thus in this study the solubility of the produced NPs and the spray dried

microparticles were measured in pH 6.8 to assess any improvement in the solubility at high pH upon nanonisation. Simulated intestinal fluid (SIF, pH 6.8) was prepared according to the USP 26th edition (2003) and made of 6.805% w/v KH_2PO_4 and 0.896% w/v NaOH. The pH value of the medium was adjusted as necessary to pH 6.8 with 0.1 M NaOH. In each experiment, excess sample (25 mg) was added to 25 ml of the SIF placed in a temperature controlled jacketed cylinder, preheated to 37 °C and continuously stirred at 1,000 rpm. Sample aliquots (1 ml) were taken and filtered through a 0.1 µm membrane filter (Sartorius Stedim, Germany) at a predetermined time intervals for 4 hours and analysed with a Shimadzu Pharmspec UV-1700 UV-Visible spectrophotometer at 262 nm without dilution using low volume 10-mm quartz cuvettes. The analysis was performed in triplicate for each sample and the average concentrations were plotted against time.

The undissolved residues were examined using PXRD to assess possible crystallisation during solubility studies.

2.9. Dissolution studies

Dissolution profiles of the stabiliser-free, PEG and MPEG stabilised ITR NPs were compared to that of the spray dried ITR microparticles. From the solubility study, after 24 hr, the solubility of crystalline ITR in FaSSGF and FaSSIF was 2.36 and 0.26 µg/ml, respectively. Therefore, 10 mg of ITR NPs or microparticles (equivalent to approximately 42 times of the solubility of crystalline ITR in FaSSGF, similar to the studies of Matteucci et al. (2009)) were added to 100 ml of FaSSGF at 37 °C with a continuous stirring using an overhead paddle with a stirring rate of 100 rpm. Aliquots were withdrawn at 5, 10, 20, 30, and 60 min and filtered using 0.1 µm membrane

filters (Sartorius Stedim, Germany). An equal volume of FaSSGF was replaced except for the 60 min sample were a concentrated solution of SIF, prepared based on an earlier experiment, was injected to shift the pH and the content of the dissolution media to that of FaSSIF and thus mimic the transition of the drug from the stomach to the small intestine. Following the pH shift, aliquots were withdrawn at 5, 10, 20, 30, 60, 120, and 180 min, filtered and an equal volume of FaSSIF was replaced. All filtered samples were diluted 3:2 v/v with the mobile phase and assayed using HPLC (Section 2.5). The analysis was performed in triplicate for each sample and the average was plotted against time. Dissolution data obtained was also used to evaluate the maximum concentration achieved, the time point at which this was achieved and the extent of supersaturation (AUC) as described before by Matteucci et al (2009).

2.10. Statistical analysis

Statistical analyses were performed via either a two sample t-test or one way ANOVA with the Tukey comparison test, as specified in relevant sections, using Minitab Release 16. For all tests, $p \leq 0.05$ was used as the criterion to assess statistical significance.

3. Results and discussion

3.1. Solubility studies

In this study, ITR NPs were precipitated from acetone using heat induced evaporative antisolvent technique (HIEAN). The particles were produced by injecting a volume of acetonic drug solution to a volume of water or an aqueous solution (antisolvent) kept at 80°C. The concentration of ITR in acetone used (6.4 mg/ml) was selected based on the solubility studies

conducted at different temperatures where the highest drug saturation was observed at 50 °C (7.34 ± 0.036 mg/ml). The concentration of the stabiliser in the antisolvent phase was chosen to be 10% relative to the drug concentration, similar to the conditions used by Liu et al. (2011). This concentration was observed here to provide the smallest particle size when PEG was used as a stabiliser and the particle size did not change significantly when this concentration was increased to 20% of the drug solubility. On the other hand, smaller particles were obtained as the concentration of MPEG in water was increased up to 1 mg/ml (Tables 1). Following this increase in MPEG concentration, there was no further size reduction observed. The solubility of crystalline ITR in the various antisolvent phases used in the HIEAN method elucidate that solubility of ITR in water at 80 °C and 25 °C was very similar and was below 0.5 μg/ml. The addition of PEG (0.64 mg/ml) and MPEG (1 mg/ml) to water increased the solubility of ITR with the 80 °C incubation temperature yielding higher solubilities (0.46 ± 0.001 and 0.61 ± 0.003 μg/ml for the aqueous PEG and MPEG solutions, respectively) than those measured at 25 °C (0.38 ± 0.003 and 0.47 ± 0.006 μg/ml). The solvent injection volumes were chosen based on results summarised in Table 1 where the formulae has the suffix NPs.

Table 1 summarises the experiments that were carried out to obtain NPs with smaller size and lower DPI values and shows that as the solvent/antisolvent ratio (v/v) increases (higher drug content is injected), larger and more polydispersed particles are produced. The 1:8 ratio v/v yielded particles in the nanometre range but they were larger than those produced when the 1:10 ratio v/v was used and since a small difference in particle size is expected to have a considerable impact on solubility and dissolution (Kondo et al. 1993), the 1:10 solvent/antisolvent (v/v) ratio was chosen. The successful production of NPs, especially the

stabiliser-free batch, can be explained with the aid of the precipitation steps described earlier and the acetone induced droplet formation reported by Re and Biscans (1998). Minute droplets are generated upon injecting the solvent phase into the antisolvent phase. This process of droplet formation is promoted by the mechanical shear forces of injection and mixing (Yang et al 2003). The very low solubility of ITR in water even at 80 °C resulting in the solidification of the droplet forming a shell enclosing the supersaturated solvent phase. The high temperature of the antisolvent permits rapid evaporation of the solvent (acetone) through the shell, solvent/antisolvent boundary, and thus the NPs are formed very quickly (Nocent et al 2001, Yang et al 2003). The rapid formation of NPs is suggested to prevent the assembly of drug molecules into the well-ordered crystal structure.

3.2 Particle size and morphology

The operating conditions used and the resulting mean particle sizes of the systems as measured by dynamic light scattering (DLS) are summarised in Table 2. The use of acetone at 50 °C as a solvent along with the use of 80 °C as the antisolvent temperature resulted in successful production of ITR NPs with mean particle sizes below 250 nm without the need of a stabiliser, thus ensures 100% drug loading, which, to the best of our knowledge, has not been reported before for ITR NPs. As it can be inferred from the SE micrographs, all produced NPs were spherical in shape with some of them displaying holes (Fig. 1a, b, c) which further supports the hypothesis of rapid solvent evaporation suggested earlier. The morphology of the NPs displayed in HeIM images was comparable to that from SEM, which excludes any artefacts due to the coating. The spray dried ITR particles were in the micron size range and possessed irregular

mushroom-like shapes as shown by SEM in Fig. 1d. The particles were highly polydisperse and could reach up to 10 µm in size.

Based on the ANOVA test, the use of PEG as a stabiliser in the antisolvent phase had a statistically significant impact on the size of the produced NPs and enabled the production of less polydisperse NPs (Table 2). Liu et al. (2011) reported that PEG is not suitable for the production of ITR nanosuspensions using milling due to the absence of any hydrophobic groups which are required for the adsorption of the stabiliser on hydrophobic drugs such as ITR. Therefore, a more hydrophobic PEG derivative, methoxylated polyethylene glycol 2000 (MPEG 2000), was used to assess any possible effects of slight chemical modification of the stabiliser on quality of produced nanoparticles. As it can be inferred from the DLS data (Table 2), the fabricated NPs had a relatively small mean particle size (although not significantly different in comparison to the PEG sample) but lower PDI compared to those produced with PEG, which is further confirmed by the SEM data (Fig. 1). It also indicates that although the solubility of ITR is higher in PEG and MPEG aqueous solutions (Table 1), the 1:10 solvent to antisolvent v/v ratio still provides the required supersaturation for the NP production.

3.3 Impact of washing, centrifugation and freeze drying

Impact of secondary NP treatment, such as washing, centrifugation and freeze drying, on morphology of NPs was assessed as these processes are often used in collection of NP-based products (Umerska et al. 2012). Table 4 presents the investigated sample handling. SE micrographs (Fig. 2a and b) of the non-washed, non-centrifuged but freeze dried sample (ITRf) illustrate micro- and nano-structures of different shapes with some hollow spheres (white

arrow) which are very close in shape to those obtained via spray drying of ITR/PEG6000/HPMC ternary dispersions (Janssens et al. 2008). Those non-uniform sample morphologies indicate that centrifugation is an essential step before freeze drying to collect the NPs. SE micrographs of the centrifuged samples illustrate that the shape and size of NPs did not exhibit any significant changes during freeze drying (Fig. 2c and d). Some of the freeze dried NPs were hollow and their surface exhibited pores, which is a common phenomenon associated with lyophilisation (Mukai et al. 2004, Wu et al. 2010). In addition, unwashed NPs showed a network-like arrangement following freeze drying (Fig. 2c, e and g), which was very close in morphology to the sample obtained by Yang et al. (2010) using ultra rapid freezing process with a ITR/mannitol solution. This network-like arrangement was not observed in the washed samples where intact and discreet NPs exhibiting better quality dominate the samples, which can be due to the removal of excess polymer and dissolved drug upon washing (Fig. 2d, f and h).

3.4 Thermal analysis

The thermal behaviour of the ITR NPs (without and with PEG or MPEG as stabilisers) as well as ITR:PEG (50:50 w/w) and ITR:MPEG (50:50 w/w) physical mixes is shown in Figure 3. The thermograms of the NPs were similar to that of the glassy ITR as described by Wang et al. (2004). The three NP samples exhibited a glass transition (Tg) event at approximately 60 °C, two endothermic transitions at 74 (T_{LC1}) and 90 °C (T_{LC2}) due to the formation of a chiral nematic mesophase (Six et al. 2001) and finally melting at ~168 °C. A crystallisation event (Tc) before melting was observable in the three samples at different temperatures. For the ITR only sample the crystallisation onset was at 105 °C and it shifted to higher temperatures in the stabilised

samples to 108 °C and 113 °C for ITR/PEG and ITR/MPEG NPs, respectively. The degree of ITR crystallinity in each sample was also calculated using Eqn. 1 and it was found that the stabiliser-free sample had the highest degree of crystalline ITR of 24±1%, followed by the PEG stabilised sample with 22±1% crystalline ITR. MPEG stabilised sample had the lowest crystalline drug content with only 16±1% crystallinity. This difference in the degree of drug crystallinity in NPs may explain the shift of the crystallisation exotherm towards lower temperatures for the 100% ITR NP sample with the highest amount of crystalline material, which acts as nuclei that accelerate crystallisation of the amorphous fraction of the sample (Lefort et al. 2004). The spray dried microparticles were 100% amorphous and exhibited a similar thermal behaviour as NPs with a Tg at 60 °C followed by two endothermic transitions at 75 and 90 °C. The crystallisation event started at 125 °C and the melting endotherm at 168 °C. This melting endotherm was broader than that reported for the glassy itraconazole (Six et al. 2001) and those recorded for our NPs (Figure 3). Therefore, a second run with a heating rate of 5 °C/min was performed. With this heating rate it was possible to observe two peaks (with onsets at 161.0 and 167.6 °C). The peak at 161 °C may be due to melting of the less stable polymorph of ITR (Six et al. 2002, Werling et al. 2007), which formed during crystallisation of amorphous, spray dried ITR. Such a peak was not detected in any of the DSC thermograms of ITR NPs, which indicates that although both microparticles and nanoparticles were liquid crystalline, their thermal behaviour was different. The second peak (at 167.6 °C) was the melting peak of the stable polymorph of ITR, as seen for NPs.

3.5 PXRD analysis

The diffractogram of the starting ITR material was characterised by sharp Bragg peaks, which confirm its crystalline structure. PXRD patterns obtained for all ITR NPs, with and without a stabiliser, revealed the presence of a single liquid crystal peak at 6.05 2θ degrees and absence of the characteristic peaks of crystalline ITR, thus confirming their disordered nature. No diffraction peaks for the polymers were detected. This was consistent with DSC data revealing either no detectable quantity of polymers bound to ITR or the presence of these polymers in an amorphous form. The first hypothesis can be excluded based on HPLC data, which proves that ITR/PEG and ITR/MPEG NP samples are not 100% ITR (drug loading of 93.91 ± 0.12 and 92.4 ± 0.47% for ITR/PEG and ITR/MPEG NPs, respectively). This suggests that both polymers were present in the amorphous form in the stabilised NPs, which was further assessed by the DSC analysis of the samples obtained following exposure to ethanol and water vapour in DVS (Section 3.8).

3.6 Determination of NP solubility

Solubility studies performed for 4 hours demonstrated that the three NP samples: the stabiliser-free and the polymer stabilised, provided higher amounts of solubilised ITR than the spray dried microparticles. MPEG stabilised NPs showed higher apparent solubility with about 20% more ITR soluble compared to the PEG stabilised NPs in the first 10 minutes and reached a steady state of 1.45 ± 0.02 μg/ml after 3 hours (Figure 5). PEG stabilised NPs showed a very close solubility profile to that of their MPEG stabilised counterparts in the first hour although they reached a steady state at lower concentrations of 1.08 ± 0.02 μg/ml after 3 hours. This can be attributed to the fact that MPEG has an OH group methoxylated which render the polymer

more hydrophobic compared to PEG, thus of a greater affinity to ITR. In addition, these NPs had a higher polymer content (Table 3). This higher percentage of polymer may have also resulted in an improved wetting of NPs. The solubility profile of the 100% ITR NPs was not far from those of the PEG and MPEG stabilised NPs in the first hour, however a lower (in comparison to the polymer containing NPs) steady state concentration of 0.79 ± 0.01 μg/ml after 3 hours was attained. In contrast, spray dried microparticles had a different solubility profile where there was a slower increase in solubility beyond 30 minutes than those observed for the NPs with a lower steady state concentration (0.54 ± 0.04 μg/ml). This superior behaviour of NPs produced using HIEAN method compared to the fully amorphous microparticles is owing to the combination of the advantages of the amorphous nature with the nanosize which led to an increase in the drug apparent solubility.

PXRD patterns obtained for the undissolved NPs that remained after the solubility studies (Fig. 6) revealed that the ITR NPs without the polymeric stabiliser had a very weak tendency to crystallise during the experiments since they produced the characteristic halo of an amorphous material with very low intensity Bragg peaks. On the other hand, the polymer (PEG or MPEG) stabilised NPs ITR had a greater tendency to crystallise as shown in Figure 6. This can be due the higher solubility of the stabilised NPs, which is due to the presence of the polymer.

3.7. Dissolution studies

ITR NPs produced using HEIAN method showed significant superiority over the spray dried microparticles during solubility investigation in high pH and dissolution studies were conducted to assess the effect of this behaviour on the dissolution properties of ITR mimicking GIT

conditions. The saturation solubility of crystalline ITR in FaSSGF is approximately 2.36 ± 0.003 μg/ml. The dissolution profile of MPEG stabilised NPs illustrates a slow release of ITR from the formulation in the first 30 minutes in FaSSGF followed by a steep increase in the dissolved ITR until a peak of 11.6 ± 0.5 μg/ml (~ 5 times solubility of crystalline ITR) is reached after 60 minutes (Figure 7). The slow release of ITR in the first 30 minutes was in accordance with the visual monitoring of the dissolution process (powder was floating on the surface for the first 30 minutes of the study) where the mixing speed of the paddle was not sufficient to wet the ITR NPs instantly. Following the pH shift, the large quantity of solubilised ITR was responsible for the sudden drop of ITR concentration in FaSSIF after 5 minutes due to the low saturation solubility of ITR in FaSSIF (approximately 0.26 ± 0.001 μg/ml). This low saturation solubility is the driving force for nucleation and growth via coagulation as described by Matteucci et al. (2009). The drop in concentration of ITR in the dissolution medium continued until the dissolved ITR reached 2.3 ± 0.2 μg/ml after 3 hours in FaSSIF, which is most likely to be due to the crystallisation of some ITR as demonstrated during the solubility study. PEG stabilised NPs yielded a peak concentration of 3.7 ± 0.7 μg/ml after 5 minutes following the switch of the dissolution media to FaSSIF (although pH of the media increased). This peak was followed by a decrease in ITR level to 2.1 ± 0.03 μg/ml, about 8 times solubility in FaSSIF, within 60 minutes. ITR only NPs exhibited a dissolution profile closely resembling that of PEG stabilised ITR NPs with a peak concentration of 2.6 ± 0.3 μg/ml achieved 5 minutes following the media pH shift. The results indicate that the absence of high supersaturation before shifting the media along with the presence of excipients in FaSSIF, compared to the MPEG stabilised NPs, prevents sudden drug precipitation following pH shift and enables to sustain the high apparent solubility

of ITR in pH=6.5. In addition, the relatively high levels of dissolved ITR from the stabilised NPs compared to the stabiliser-free NPs in the FaSSGF support the hypothesis of amorphous drug present along with amorphous polymer on the surface of the NPs. This amorphous ITR is wetted and dissolved in FaSSGF yielding 1.4 ± 0.01 and 1.2 ± 0.09 μg/ml of ITR in the first 30 minutes from the MPEG and PEG stabilised NPs, respectively. Spray dried microparticles exhibited the lowest peak maximum (0.4 ± 0.01 μg/ml) 5 minutes following pH shift. This indicates that size reduction and thus an increase in powder surface area had a greater effect on dissolution properties of ITR in comparison to the solid state effects as the MPs were fully amorphous compared to the NPs (Leuner et al. 2000). A decrease in ITR concentration to 0.14 ± 0.02 μg/ml occurred within 60 minutes for ITR MPs following pH shift to 6.5. This can be explained by the partial crystallisation observed from the PXRD analysis of the undissolved microparticles remained following solubility study.

To get an insight into the total amount of ITR released throughout the dissolution study, the area under the curve (AUC) for each of the four samples was calculated and the results, along with maximum concentration achieved, expressed here as C_{max} for lucidity, are presented in Table 5. A two sample t-test was also carried out for AUC and C_{max}. From the AUC data it can be inferred that the soluble ITR available in the dissolution media from the MPEG stabilised NPs was twice that of the PEG stabilised batch. The polymer-free NPs and the spray dried microparticles provided considerably less soluble ITR. The effect of size reduction is demonstrated by the higher AUC of the stabiliser-free NPs compared to the MPs. However, the presence of a small quantity of polymer has a greater implication on the solubility than does the size only as indicated by the approximately twelve fold greater AUC of the MPEG stabilised

NPs compared to their stabiliser-free counterparts. Statistical analysis indicates that all AUC and C_{max} values calculated for all the samples were statistically significantly different. The type of the polymer included had a significant impact on the behaviour of the NPs in the dissolution studies as can be inferred from the improvement in AUC and C_{max} associated with the exchange of PEG by MPEG in the NPs, although there was no significant difference in the size of the produced NPs as indicated earlier (Table 2).

3.8. Dynamic vapour sorption

In Figure 8, DVS isotherms of a full cycle of sorption-desorption of the spray dried amorphous ITR and the ITR NPs in ethanol vapour are displayed. The isotherms revealed that the spray dried amorphous ITR (MPs), when exposed to a series of 10% step changes of ethanol vapour from 0 to 90% P/P_0, gained a mass of 4.29 ± 0.21% of its dry weight up to 80% P/P_0 followed by a mass loss of 3.66 ± 0.35% in the 80-90% P/P_0 step. A lower mass gain, 3.41 ± 0.13% at 70% ethanol vapour in the sorption cycle, was showed by the ITR NPs produced using the HEIAN method, which indicates that they are less stable than the spray dried powder. Another mass gain of 0.16 ± 0.03% occurred by the end of the sorption cycle (between 80 and 90% P/P_0). The PEG and the MPEG stabilised NPs were characterised by a mass gain of 2.73 ± 0.12 and 2.53 ± 0.07% up to 60% P/P_0, respectively, followed by a mass loss (2.16 ± 0.08 and 1.61 ± 0.13%) in the 60-70% ethanol vapour step.

According to DVS data, the spray dried ITR sorbed more ethanol vapour than the other samples because it was a fully amorphous material unlike the NPs produced by the HIEAN method where the crystalline content could act as nuclei for crystallisation. Among the NPs, although

they are less amorphous based on DSC data, the stabiliser-free NPs absorbed more ethanolic vapour than did the polymer stabilised NPs. This could be because the latter contain either PEG or MPEG, which also attract the ethanol vapour. All samples were fully crystalline after one sorption-desorption cycle upon examination by PXRD and DSC, where the characteristics crystalline ITR PXRD patterns and the sharp endotherm at 168 °C in DSC thermograms were observed. In the polymer stabilised samples there was a small endotherm observed at 52 °C, which is most likely the characteristic melting peak of PEG or MPEG. This supports the hypothesis (stated earlier in Section 3.5) of the presence of amorphous polymers in the NPs, which crystallised upon exposure to ethanol vapour.

The moisture sorption-desorption isotherms using water vapour for the ITR NPs at 25 and 50 °C are illustrated in Figure 9 a, b, and c. All isotherms at 25 °C have a hysteresis, where the water content at each relative humidity step is higher during desorption than sorption. The condensed water on the surface can act as a driving force for water penetration which is not applicable for desorption (York 1981). In addition, in the PEG and MPEG stabilised NPs, the presence of a small quantity of the hygroscopic polymer can also attract more water during the sorption cycle and retain it during the desorption, which makes a greater hysteresis effect in isotherms of the stabilised NPs. This also explains the higher water uptake (mass gain) observed in the polymer stabilised NPs (2.63% and 2.59% for ITR/PEG and ITR/MPEG at 90% RH, respectively) compared to 2.00% for the polymer-free NPs. The effect of the hygroscopic polymer can be also inferred from the final weight of the sample after the sorption/desorption cycle, which is higher than that of the initial sample mass in the case of the polymer stabilised NPs, where the polymer retained a higher quantity of water compared to the polymer-free NPs,

where no observable weight gain was found at the end of the desorption cycle. There were no pores observed in the SE micrograph of the spray dried sample (Fig. 1) and this, in combination with the lower surface area of MPs, might explain the lower hysteresis effect compared to that of the NPs (Columbano et al. 2002). The total mass gain (water uptake) was also lower in the spray dried sample, 1.8% at 90% RH.

The moisture sorption and desorption isotherms generated with water vapour at 50 °C were type III isotherm according to the IUPAC system (Airaksinen et al. 2005) and characteristic of a weak adsorbate-adsorbent interaction which is consistent with the hydrophobic nature of ITR. The isotherms illustrate mass gains in all samples due to water uptake (Figure 9). The percentage of mass gain was different for each sample. In general, NPs exhibited lower mass gains compared to MPs. The maximum uptake among the NPs was by the PEG stabilised sample, which was also characterised by the highest uptake at 25 °C (squares in Figure 9). In addition, there was a very small hysteresis effect observed all of the isotherms obtained for the NP samples indicating that water sorption under these conditions was completely reversible, which can be attributed to analysis of the samples at 50 °C, which may facilitate water evaporation during desorption. Unlike the 25 °C data, the 50 °C isotherms of MPs indicate the highest weight gain in comparison to all samples investigated (about 2.49 ± 0.04 % of its dry weight at 90% RH).

DSC and PXRD examination of all samples subjected to water vapour showed that all samples were still amorphous following exposure to water vapour at 25 °C in DVS. A slight shift in the crystallisation exothermic peak temperature in DSC was observed for all samples. The MPEG stabilised sample, which appeared to have the highest crystallisation temperature was found to

have the lowest crystallisation onset following DVS analysis (94 ± 0.3 °C), followed by the PEG stabilised NPs which crystallised at 98.9 ± 0.1 °C (onset). In both samples a melting peak at 52 °C was observed due to crystallised polymer. The stabiliser-free sample was the most stable among the NP samples and crystallised at 104.2 ± 0.3 °C (onset). The spray dried MPs were less affected by the exposure to water vapour at 25 °C in DVS and crystallisation started at 125.2 ± 0.3 °C. The above observations illustrate the effect of polymer crystallisation on thermal stability of the NPs, where the entrapment of water and rearrangement of polymer molecules facilitate ITR crystallisation at lower temperatures compared to the polymer-free samples. Similarly, all samples exhibited the halo pattern with a single liquid crystal peak upon examination using PXRD, consistent with DSC data.

Upon elevation of the DVS analysis temperature to 50 °C, a further decrease in the crystallisation onset temperature was recorded for all nanoparticulate samples (ITR NPs = 97.9 ± 0.4, ITR/PEG NPs = 97.1 ± 0.5, ITR/MPEG = 93.2 ± 0.7 °C). On the other hand, when examined by PXRD, in the polymer stabilised NPs there were some residual peaks emerging from the halo pattern along with the single liquid crystal peak, which further explains the crystallisation peak shift to lower temperatures in DSC. These residual crystalline peaks where hardly detected in the stabiliser-free NPs and the spray dried microparticles. On the other hand, the liquid crystal peak was nearly invisible in the diffractogram of microparticles, which could indicate a phase change. DSC thermogram showed a crystallisation onset at a lower temperature, 120.1 ± 0.3 °C of the DVS sample compared to 125 ± 0.9 °C for the untreated ITR MPs and the enthalpy of melting of the metastable polymorph was slightly greater than that of the material before DVS experiment. Collectively, observations from DVS at 50 °C, DSC and PXRD suggest a possible

structural collapse in part of the amorphous MP sample during the DVS cycle. Structural collapse before crystallisation was reported by Buckton and Darcy (1996), where exposure to 40% and 50% RH induced structural changes but not crystallisation of lactose.

4. Conclusions

The heat induced evaporative antisolvent nanoprecipitation (HIEAN) of ITR from acetone at 80 °C produces primarily amorphous NPs with the mean particle size less than 250 nm and 100% drug loading. These NPs demonstrated greater solubility and improved dissolution profile compared to the spray dried amorphous ITR microparticles. Smaller NPs with lower polydispersity indices can be obtained when polyethylene glycol or its methoxylated derivative is included in the antisolvent phase as a stabiliser. Enhanced dissolution was associated with the use of MPEG as a stabiliser. In all samples, washing appears to improve the quality of the produced NPs. Centrifugation was found to be an essential step for the collection of NPs, otherwise a mixture of particles with different shapes and sizes were obtained. The stabilising polymer was in an amorphous state as evidenced by PXRD, DSC and DVS studies. Analysis indicates that there was no significant change in the solid state properties of ITR NPs when subjected to water vapour up to 90% RH at 25 °C with an increase in the crystallinity in the polymer stabilised samples if temperature was increased to 50 °C.

5. Acknowledgements

This work was funded by the Libyan ministry of higher education and scientific research through the Libyan Embassy, London and supported by the Science Foundation Ireland under Grant No. 12/RC/2275 (Synthesis and Solid State Pharmaceuticals Centre). The authors would like to

thank Dr. Grzegorz Garbacz (Physiolution GmbH, Germany) for kindly supplying itraconazole and Centre for Research on Adaptive Nanostructures and Nanodevices (CRANN, TCD) for performing HeIM imaging.

References:

Airaksinen, S., Karjalainen, M., Shevchenko, A., Westermarck, S., Leppänen, E., Rantanen, J., Yliruusi, J., 2005. Role of water in the physical stability of solid dosage dormulations. J. Pharm. Sci. 94, 2147–2165.

Badawi, A.A., El-Nabarawi, M.A., El-Setouhy, D.A., Alsammit, S.A., 2011. Formulation and stability testing of itraconazole crystalline nanoparticles. AAPS Pharm. Sci. Tech. 12, 811–820.

Barrett, A.M., Dehghani, F., Foster, N.R., 2008. Increasing the dissolution rate of itraconazole processed by gas antisolvent techniques using polyethylene glycol as a carrier. Pharm. Res. 25, 1274–1289.

Beck, C., Dalvi, S.V., Dave, R.N., 2010. Controlled liquid antisolvent precipitation using a rapid mixing device. Chem. Eng. Sci. 65, 5669–5675.

Bosselmann, S., Nagao, M., Chow, K.T., Williams III, R.O., 2012. Influence of formulation and processing variables on properties of itraconazole nanoparticles made by advanced evaporative precipitation into aqueous solution. AAPS Pharm. Sci. Tech. 13, 949–960.

Buckton, G., Darcy, P., 1996. Water mobility in amorphous lactose below and close to the glass transition temperature. Int. J. Pharm. 136, 141–146.

Chen, J.F., Zhang, J.Y., Shen, Z.G., Zhong, J., Yun, J., 2006. preparation and characterization of amorphous cefuroxime axetil drug nanoparticles with novel technology: high-gravity antisolvent precipitation. Ind. Eng. Chem. Res. 45, 8723–8727.

Chen, W., Gu, B., Wang, H., Pan, J., Lu, W., Hou, H., 2008. Development and evaluation of novel itraconazole-loaded intravenous nanoparticles. Int. J. Pharm. 362, 133–140.

Chen, X., Benhayoune, Z., Williams, R.O., Johnston, K.P., 2004. Rapid dissolution of high potency itraconazole particles produced by evaporative precipitation into aqueous Solution, J. Drug Deliv. Sci. Technol. 14, 299–304.

Chen, X., Young, T.J., Sarkari, M., Williams III, R.O., Johnston, K.P., 2002. Preparation of cyclosporine A nanoparticles by evaporative precipitation into aqueous solution. Int. J. Pharm. 242, 3–14.

Chow, A., Tong, H., Chattopadhyay, P., Shekunov, B., 2007. Particle engineering for pulmonary drug delivery. Pharm. Res. 24, 411–437.

Columbano, A., Buckton, G., Wikeley, P., 2002. A study of the crystallisation of amorphous salbutamol sulphate using water vapour sorption and near infrared spectroscopy. Int J. Pharm. 237, 171–178.

Dalvi, S.V., Dave, R.N., 2010. Analysis of nucleation kinetics of poorly water-soluble drugs in presence of ultrasound and hydroxypropyl methyl cellulose during antisolvent precipitation. Int. J. Pharm. 387, 172–179.

Dressman, J.B., Reppas, C., 2000. In vitro-in vivo correlations for lipophilic, poorly water-soluble drugs. Eur. J. Pharm. Sci. 11, S73–S80.

Gardner, C.R., Walsh, C.T., Almarsson, O., 2004. Drugs as materials: valuing physical form in drug discovery. Nat. Rev. Drug Discov. 3, 926–934.

Hancock, B. C., Parks, M., 2000. What is the true solubility advantage for amorphous pharmaceuticals. Pharm. Res. 17, 397–404.

Janssens, S., De Armas, H.N., Roberts, C.J., Van Den Mooter, G., 2008. Characterization of ternary solid dispersions of itraconazole, PEG 6000, and HPMC 2910 E5. J. Pharm. Sci. 97, 2110–2120.

Jones, A.G., Mullin, J.W., 1974. Programmed cooling crystallization of potassium sulphate solutions, Chem. Eng. Sci. 29, 105–118.

Kapsi, S.G., Ayres, J.W., 2001. Procesing factors in development of solid solution formulation of itraconazole for enhancement of drug dissolution and bioavailability. Int. J. Pharm. 229, 193–203.

Keck, C.M., Müller R.H., 2006. Drug nanocrystals of poorly soluble drugs produced by high pressure homogenisation. Eur. J. Pharm. Biopharm. 62, 3–16.

Kondo, N., Iwao, T., Masuda, H., Yamanouchi, K., Ishihara, Y., Yamada, N., Haga, T., Ogawa, Y. and Yokoyama, K., 1993. Improved oral absorption of a poorly water-soluble drug, HO-221, by wet-bead milling producing particles in submicron region. Chem. Pharm. Bull. 41, 737–740.

Kumar, V., Wang, L., Riebe, M., Tung, H.H., Prud'homme, R.K., 2009. Formulation and stability of itraconazole and odanacatib nanoparticles: Governing physical parameters. Mol. Pharm. 6, 1118–1124.

Lee, M.K., Kim, S., Ahn, C.H., Lee, J., 2010. Hydrophilic and hydrophobic amino acid copolymers for nano-comminution of poorly soluble drugs. Int. J. Pharm. 384, 173–180.

Lefort, R., De Gusseme, A., Willart, J.F., Danède, F., Descamps, M., 2004. Solid state NMR and DSC methods for quantifying the amorphous content in solid dosage forms: an application to ball-milling of trehalose. Int. J. Pharm. 280, 209–219.

Leuner, C., Dressman, J., 2000. Improving drug solubility for oral delivery using solid dispersions. Eur. J. Pharm. Biopharm. 50, 47–60.

Liu, P., Rong, X., Laru, J., Veen, B., Kiesvaara, J., Hirvonen, J., Laaksonen, T., Peltonen, L., 2011. Nanosuspensions of poorly soluble drugs: preparation and development by wet milling. Int. J. Pharm. 411, 215–222.

Liversidge, G.G., Cundy, K.C., 1995. Particle size reduction for improvement of oral bioavailability of hydrophobic drugs. I Absolute oral bioavailability of nanocrystalline danazole in beagle dogs. Int. J. Pharm. 127, 91–97.

Matteucci, M.E., Hotze, M.A., Johnston, K.P., Williams, R.O., 2006. Drug nanoparticles by antisolvent precipitation: Mixing energy versus surfactant stabilization. Langmuir. 22, 8951–8959.

Matteucci, M.E., Paguio, J.C., Miller, M.A., Williams, R.O., Johnston, K.P., 2009. Highly supersaturated solutions from dissolution of amorphous itraconazole microparticles at pH 6.8. Mol. Pharm. 6, 375–385.

Miller, M.A., DiNunzio, J., Matteucci, M.E., Ludher, B.S., Williams, R.O., Johnston, K.P., 2012. Flocculated amorphous itraconazole nanoparticles for enhanced in vitro supersaturation and in vivo bioavailability. Drug Dev. Ind. Pharm. 38, 557–570.

Mukai, S.R., Nishihara, H., Shichi, S., Tamon, H., 2004. Preparation of porous TiO2 cryogel fibers through unidirectional freezing of hydrogel followed by freeze-drying. Chem. Mater. 16, 4987–4991.

Mullin, J.W., Nývlt, J., 1971. Programmed cooling of batch crystallizers, Chem. Eng. Sci. 26, 369–377.

Odds, F.C., Oris, M., Van Dorsselaer, P., Van Gerven, F., 2000. Activities of an intravenous formulation of itraconazole in experimental disseminated *Aspergillus*, *Candida*, and *Cryptococcus* infections. Antimicrob. Agents Chemother. 44, 3180–3183.

Owen, H., Graham, S., Werling, J.O., Carter, P.W., 2009. Anion effects on electrostatic charging of sterically stabilized, water insoluble drug particles. Int. J. Pharm. 368, 154–159.

Paluch, K.J., Tajber, L., McCabe, T., O'Brien, J.E., Corrigan, O.I., Healy, A.M., 2010. Preparation and solid state characterisation of chlorothiazide sodium intermolecular self-assembly suprastructure. Eur. J. Pharm. Sci. 41, 603-611.

Re`, M.I., Biscans, B., 1998. Preparation of microspheres of ketoprofen with acrylic polymers by a quasi-emulsion solvent diffusion method. Powder Technol. 101, 120–133.

Saag, M.S., Dismukes, W.E., 1988. Azole antifungal agents: Emphasis on new triazoles. antimicrob. Agents Chemother. 32, 1–8.

Shah, B., Kakumanu, V., Bansal, A., 2006. Analytical techniques for quantification of amorphous/crystalline phases in pharmaceutical solids. J. Pharm. Sci. 95, 1641–1665

Shah, P., 2006. Use of nanotechnologies for drug delivery, MRS Bulletin. 31, 894–899.

Six, K., Verreck, G., Peeters, J., Binnemans, K., Berghmans, H., Augustijns, P., Kinget, R., Van den Mooter, G., 2001. Investigation of thermal properties of glassy itraconazole: identification of a monotropic mesophase. Thermochem. Acta. 376, 175–181.

Six, K., Leuner, C., Dressman, J., Verreck, G., Peeters, J., Blaton, N., Augustijns, P., Kinget, R., Van den Mooter, G., 2002. Thermal properties of hot-stage extrudates of itraconazole and eudragit E100. Phase separation and polymorphism. J. Therm. Anal. Cal. 68, 591–601

Tam J.M., Engstrom, J.D., Ferrer, D., Williams, R.O., Johnston, K.P., 2010. Templated open flocs of anisotropic particles for pulmonary delivery with pressurized metered dose inhalers. J. Pharm. Sci. 99, 3150–3165.

United States Pharmacopeia and National Formulary, United States Pharmacopeial Convention Inc., Rockville, MD, USA, 26th Edition (2003).

Umerska, A., Paluch, K.J., Inkielewicz-Stepniak, I., Santos-Martinez, M.J., Corrigan, O.I., Medina, C., Tajber, L., 2012. Exploring the assembly process and properties of novel crosslinker-free hyaluronate-based polyelectrolyte complex nanocarriers. Int. J. Pharm. 436, 75-87.

Van Eerdenbrugh, B., Van den Mooter, G., Augustijns, P., 2008. Top-down production of drug nanocrystals: Nanosuspension stabilization, miniaturization and transformation into solid products. Int. J. Pharm. 364, 64–75.

Wang, X., Michoel, A., Mooter, G.V., 2004. Study of phase behaviour of polyethylene glycol 6000-itraconazole solid dispersion using DSC. Int. J. Pharm. 272, 181–187.

Weers, J.G., Tarara, T.E., Clark, A.R., 2007. Design of fine particles for pulmonary drug delivery. Expert Opinion on Drug Deliv. 4, 297–313.

Werling, J., Doty, M.J., Rebbeck, C.L., Wong, J.C.T., Kipp, J.E., 2007. Polymorphic Form of Itraconazole. U.S Patent: 7193084.

Wiedmann, T.S., DeCastro, L., Wood, R.W., 1997. Nebulization of NanoCrystals^{TM}: Production of a respirable solid-in-liquid-in-air colloidal dispersion. Pharm. Res. 14, 112–116.

Wu, X., Liu, Y., Li, X., Wen, P., Zhang, Y., Long, Y., Wang, X., GuoY., Xing, F., Gao, J., 2010. Preparation of aligned porous gelatin scaffolds by unidirectional freeze-drying method. Acta Biomaterialia. 6, 1167–1177.

Yang, W., Keith P. Johnston, K.P., Williams III, R.O., 2010. Comparison of bioavailability of amorphous versus crystalline itraconazole nanoparticles via pulmonary administration in rats. Eur. J. Pharm. Biopharm. 75, 33–41.

York, P., 1981. Analysis of moisture sorption hysteresis in hard gelatin capsules, maize starch, and maize starch: drug powder mixtures. J. Pharm. Pharmacol. 33, 269–273.

Table 1. Outline of trial experiments, which were done to optimise the precipitation conditions and the size of NPs. PDI – polydispersity index, SD – standard deviation.

Formula	PEG conc. (mg/ml)	MPEG conc. (mg/ml)	Solvent/antisolvent (v/v) ratio	Mean particle size ± SD (nm)	PDI ± SD
ITR only	0	0	1:8	797 ± 56	0.053 ± 0.040
ITR only	0	0	1:6.7	1489 ± 168	0.156 ± 0.078
ITR only	0	0	1:5	1708 ± 423	0.782 ± 0.377
ITR only NPs*	0	0	1:10	240 ± 3	0.087 ± 0.014
ITR PEG	0.64	0	1:8	780 ± 52	0.174 ± 0.042
ITR PEG	0.64	0	1:6.7	1169 ± 195	0.221 ± 0.078
ITR PEG	0.64	0	1:5	1539 ± 337	0.290 ± 0.170
ITR PEG NPs*	0.64	0	1:10	221 ± 2	0.041 ± 0.007
ITR PEG	1.00	0	1:10	222 ± 3	0.038 ± 0.011
ITR MPEG	0	0.64	1:10	220± 4	0.048 ± 0.025
ITR MPEG	0	0.64	1:8	378 ± 19	0.106 ± 0.054
ITR MPEG	0	0.64	1:6.7	609 ± 108	0.174 ± 0.038
ITR MPEG	0	0.64	1:5	794 ± 129	0.388 ± 0.237
ITR MPEG NPs*	0	1.00	1:10	216 ± 0.4	0.011 ± 0.007

* - final formulations selected for further testing

Table 2. Manufacturing and separation conditions employed to optimise the quality of produced particles. In all cases the solvent and antisolvent temperatures were 50 and 80 °C, respectively, and a 1:10 solvent/antisolvent (v/v) ratio was used.

Sample	Stabiliser conc. (mg/ml)	Stabiliser phase	Centrifugation	Washing	Freeze drying
ITRf	N/A	N/A	No	No	Yes
ITRcf	N/A	N/A	Yes	No	Yes
ITRwcf	N/A	N/A	Yes	Yes	Yes
ITR/PEGcf	0.64	Antisolvent	Yes	No	Yes
ITR/PEGwcf	0.64	Antisolvent	Yes	Yes	Yes
ITR/MPEGcf	1.00	Antisolvent	Yes	No	Yes
ITR/MPEGwcf	1.00	Antisolvent	Yes	Yes	Yes

Table 3. Summary of the EOS (extent of supersaturation), C_{max} (maximum concentration), T_{max} (time to maximum concentration) parameters obtained from the dissolution studies. SD – standard deviation.

Sample	$EOS_{0\text{-}240min}$ ± SD (μg·min/ml)	C_{max} ± SD (μg/ml)
ITR NPs	68.0 ± 2.9	2.6 ± 0.3
ITR/PEG NPs	469.2 ± 7.6	3.7 ± 0.7
ITR/MPEG NPs	843.1 ± 24.6	11.6 ± 0.5
SD MPs	30.7 ± 3.6	0.4 ± 0.01

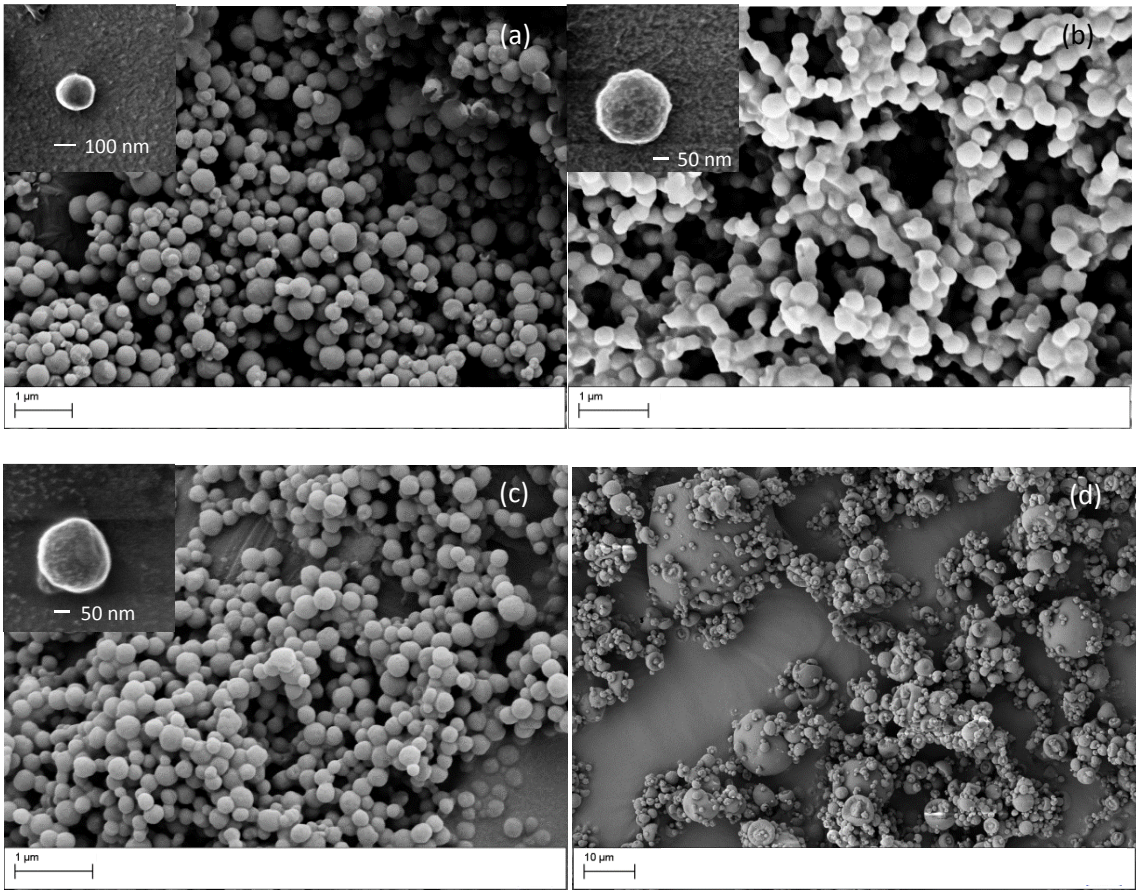

Figure 1. SE micrographs and HeI micrographs (in the upper left corner of SE micrographs for NPs) of: (a) stabiliser-free ITR NPs, (b) PEG stabilised NPs, (c) MPEG stabilised NPs and (d) spray dried ITR microparticles.

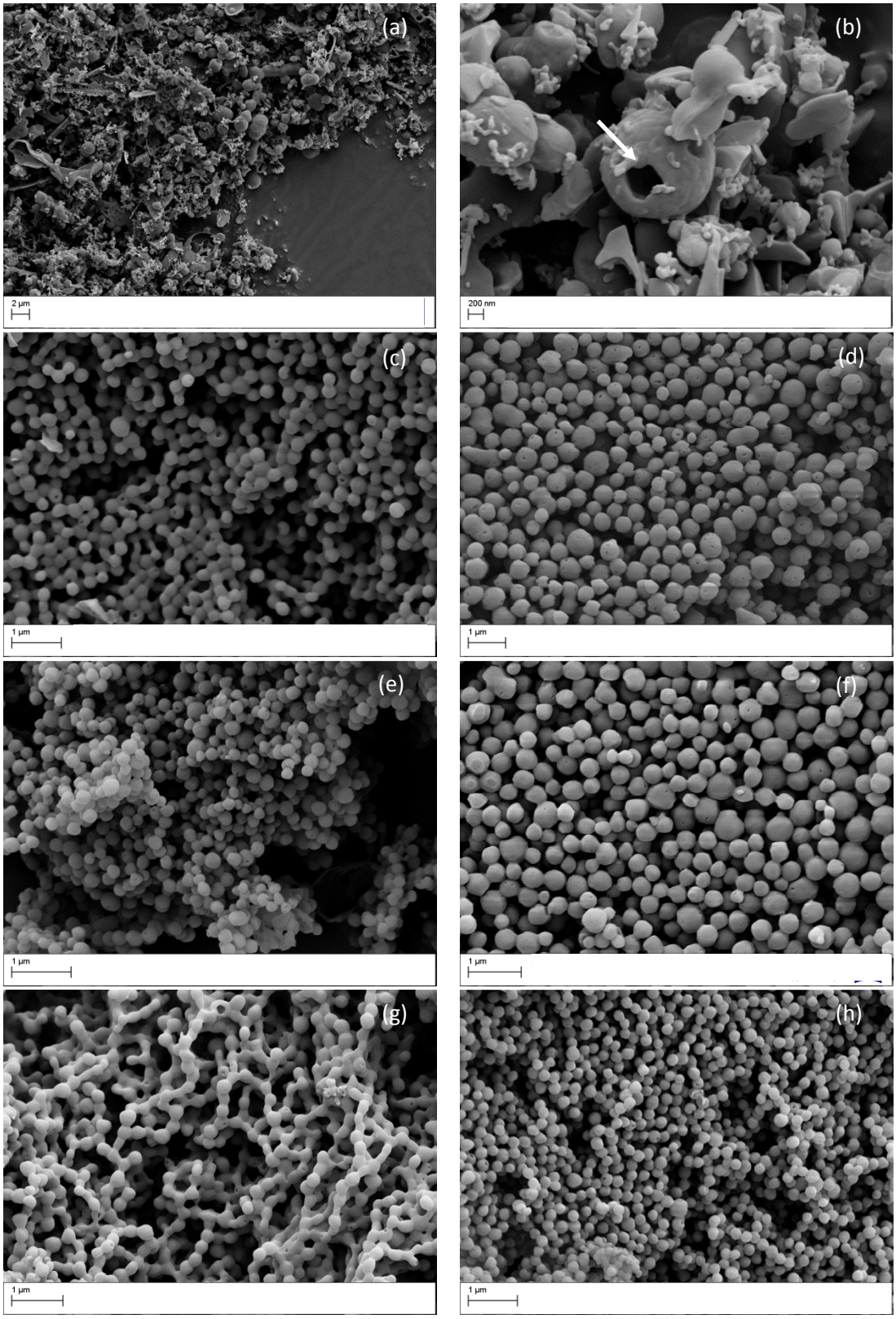

Figure 2. Scanning electron micrographs of (a, b) ITRf NPs (c) ITRcf NPs, (d) ITRwcf NPs, (e) ITR/PEGcf NPs (f) ITR/PEGwcf NPs, (g) ITR/MPEGcf NPs and (h) ITR/MPEGwcf NPs. White arrow shows an apparent hole in the nanoparticle, sample codes are explained in Table 4.

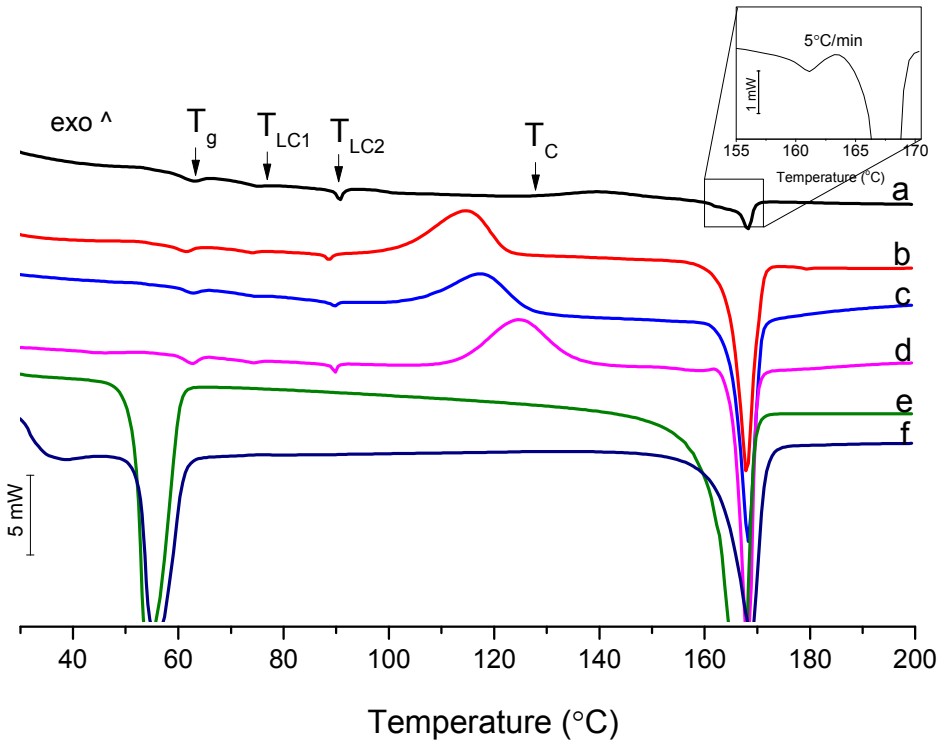

Figure 3. DSC thermograms of: (a) spray dried ITR MPs, (b) stabiliser-free ITR NPs, (c) PEG stabilised NPs, (d) MPEG stabilised NPs, (e) ITR and PEG 50:50 (w/w) physical mix and (f) ITR and MPEG 50:50 (w/w) physical mix. Tg – glass transition, T_{LC1} and T_{LC2} – events associated with liquid crystalline transitions and T_C – onset of crystallisation.

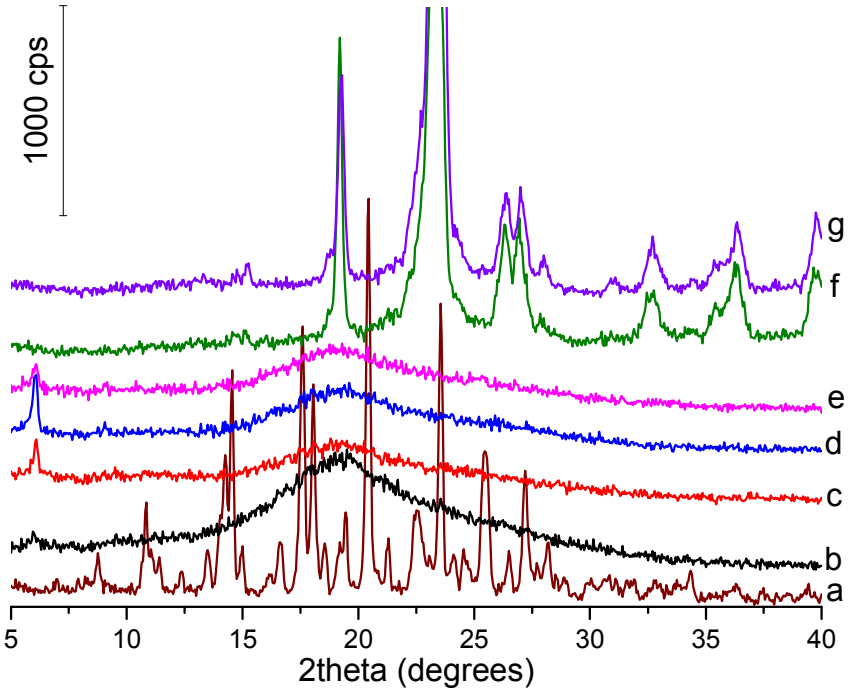

Figure 4. PXRD diffraction patterns of (a) crystalline ITR, (b) spray dried microparticles, (c) stabiliser-free ITR NPs, (d) PEG stabilised NPs, (e) MPEG stabilised NPs, (f) crystalline PEG and (g) crystalline MPEG.

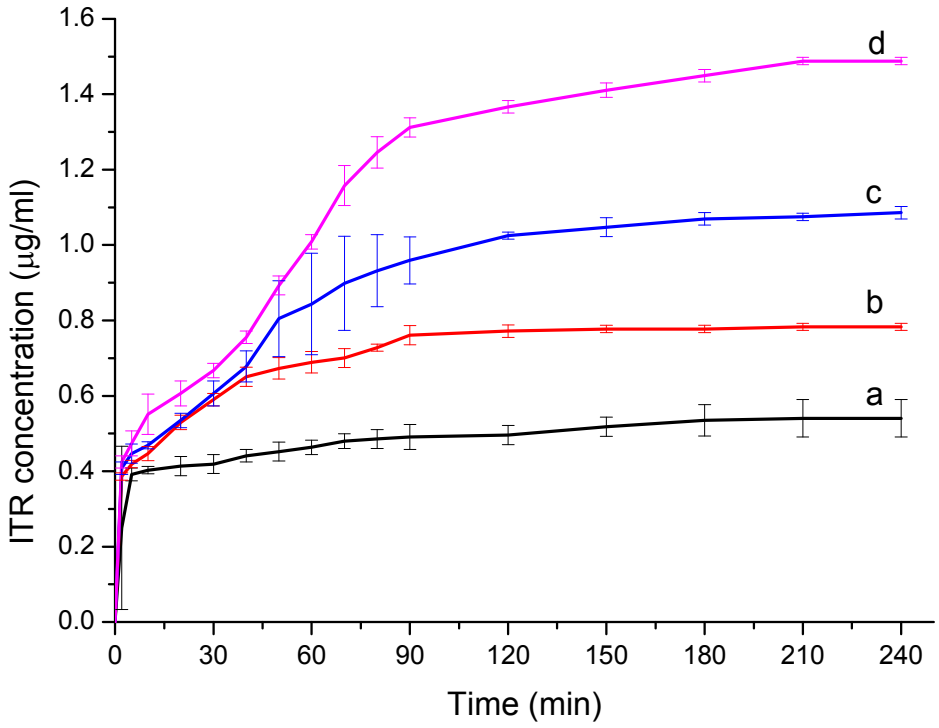

Figure 5. Solubility profiles of (a) spray dried microparticles, (b) stabiliser-free ITR NPs, (c) PEG stabilised NPs and (d) MPEG stabilised NPs.

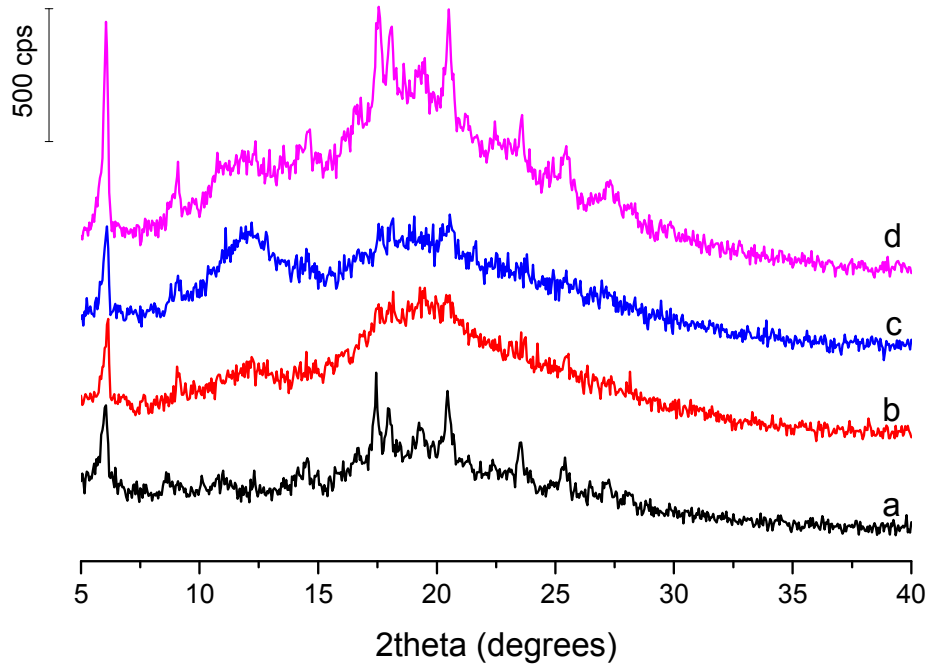

Figure 6. PXRD patterns of the remaining undissolved powders following solubility studies of (a) spray dried microparticles, (b) stabiliser-free ITR NPs, (c) PEG stabilised NPs and (d) MPEG stabilised NPs.

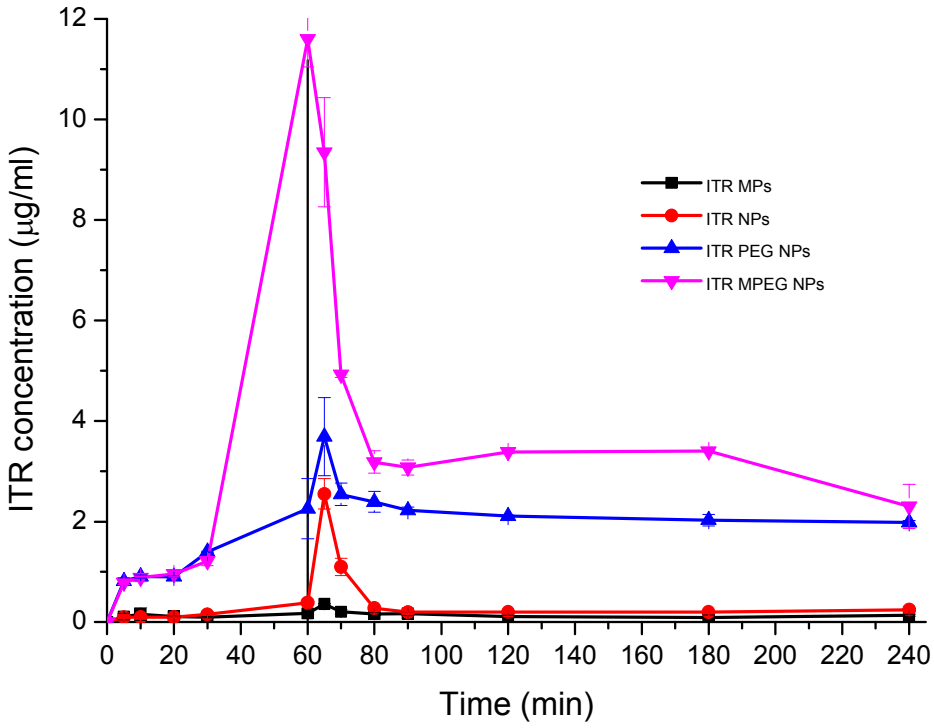

Figure 7. Dissolution profiles of ITR nano- and micro-particles. The vertical line indicates dissolution media change from FaSSGF to FaSSIF.

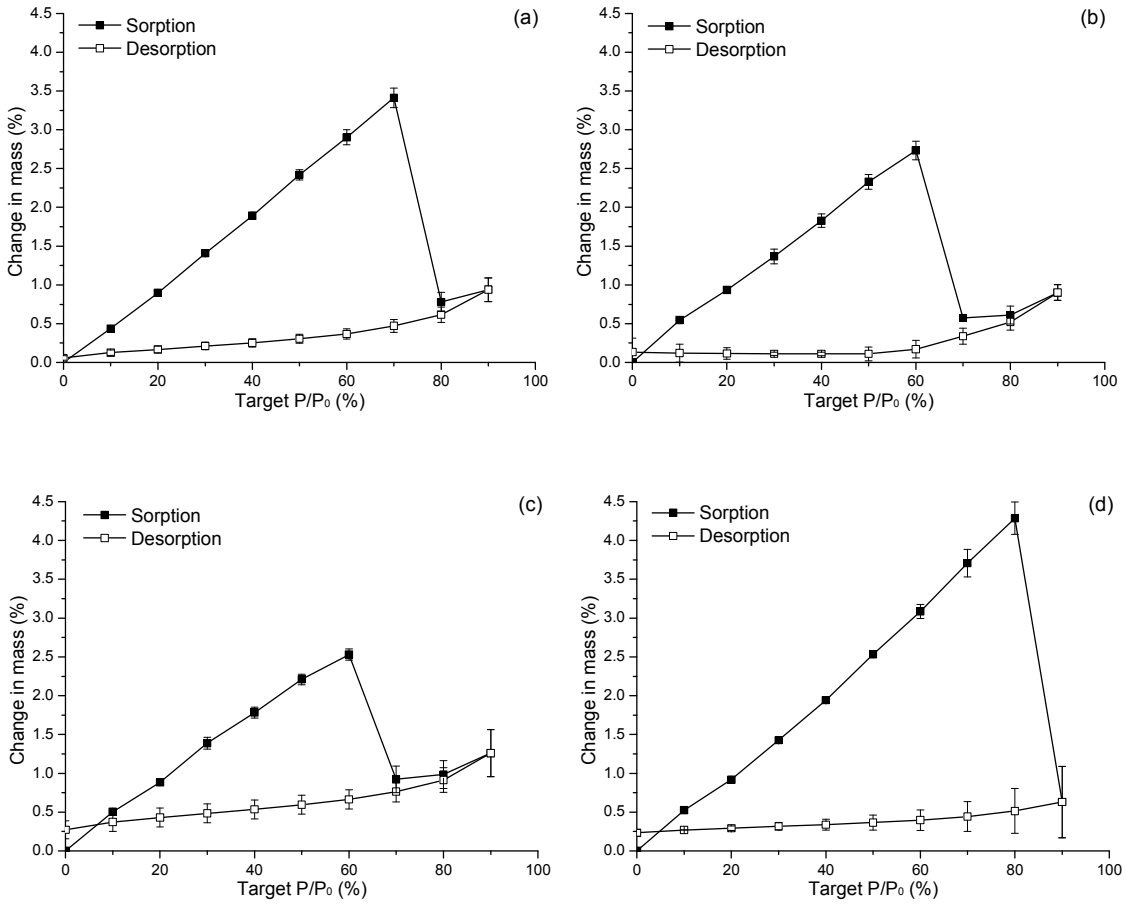

Figure 8. DVS sorption-desorption isotherm of (a) stabiliser-free ITR NPs, (b) PEG stabilised ITR NPs, (c) MPEG stabilised ITR NPs, and (d) spray dried ITR MPs. Experiments were carried out at 25 °C using ethanol.

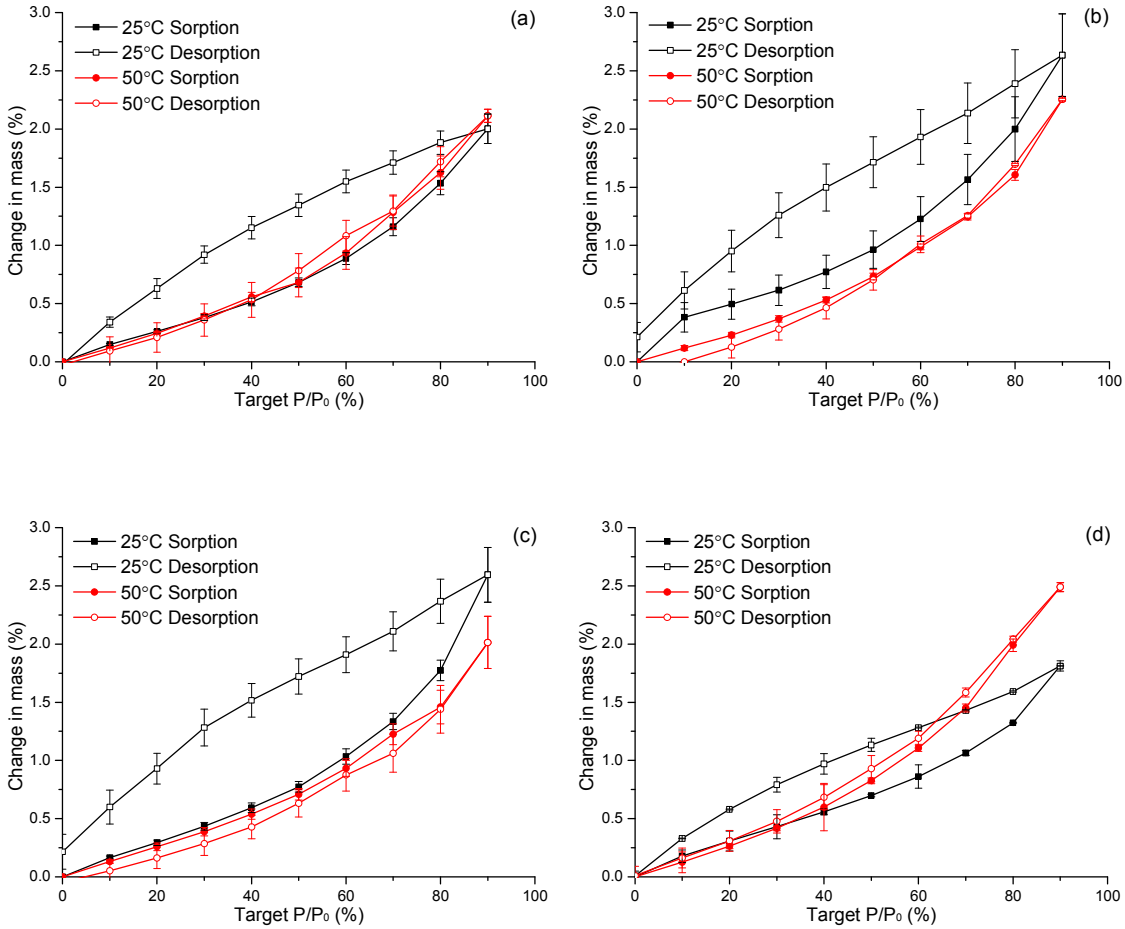

Figure 9. DVS sorption-desorption isotherm of (a) stabiliser-free ITR NPs, (b) PEG stabilised ITR NPs (c) MPEG stabilised ITR NPs and (d) SD ITR MPs. Experiments were carried out at 25 and 50 °C using water.